La matière noire dans les galaxies à grand z

A. Bosma
Observatoire de Marseille – LAM/OAMP

z = 2 ? les galaxies ne sont pas encore suffisamment établies

z = 1 ? il y a des graves problèmes de résolution angulaire

z = 0.5 alors ? Peut-être SKA + ALMA + JWST NIRSpec

z = 0.2 : pour rester modeste, mais réaliste

z = 0.0 : on ne comprend pas tout, mais pas du tout,
donc il y a encore du travail à faire ...

Millenium Simulation

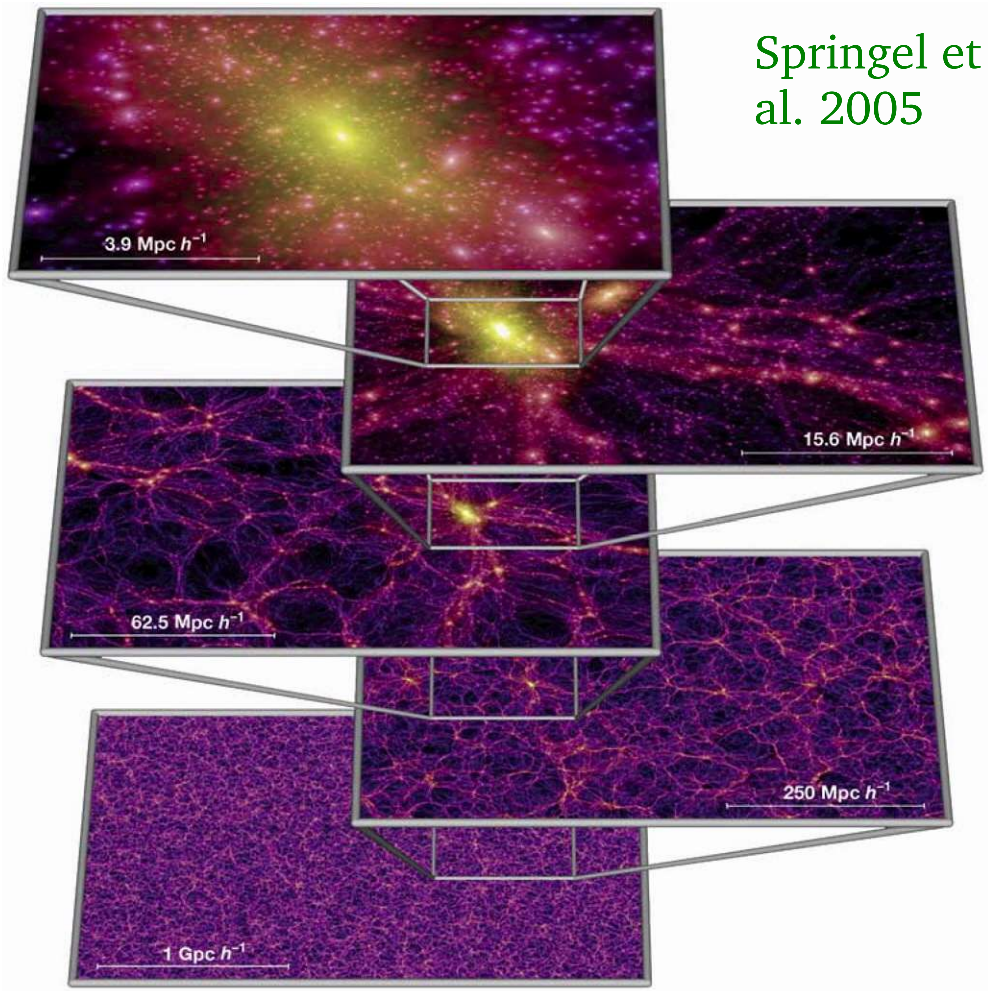

Springel et al. 2005

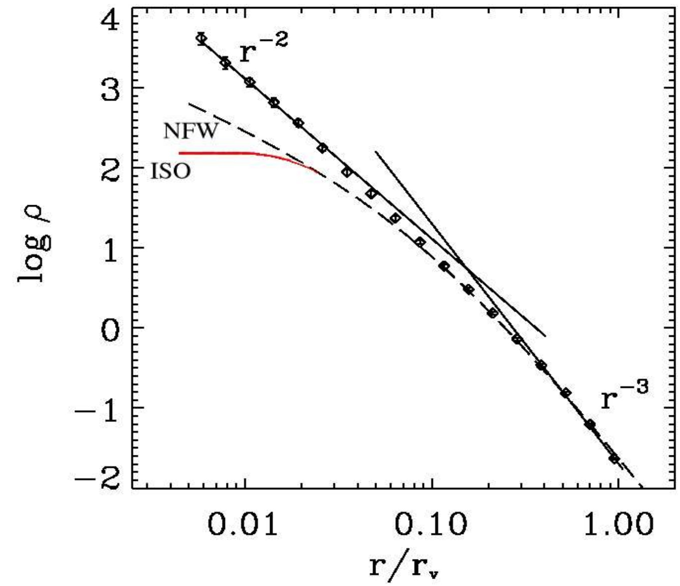

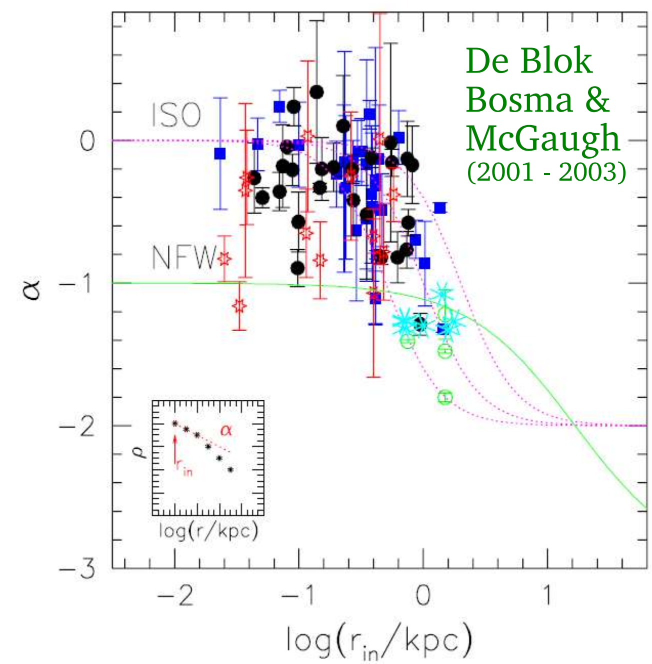

ΛCDM has problems on galaxy scales

cuspy halos
lots of satellites

core/cusp debate (at z=0)

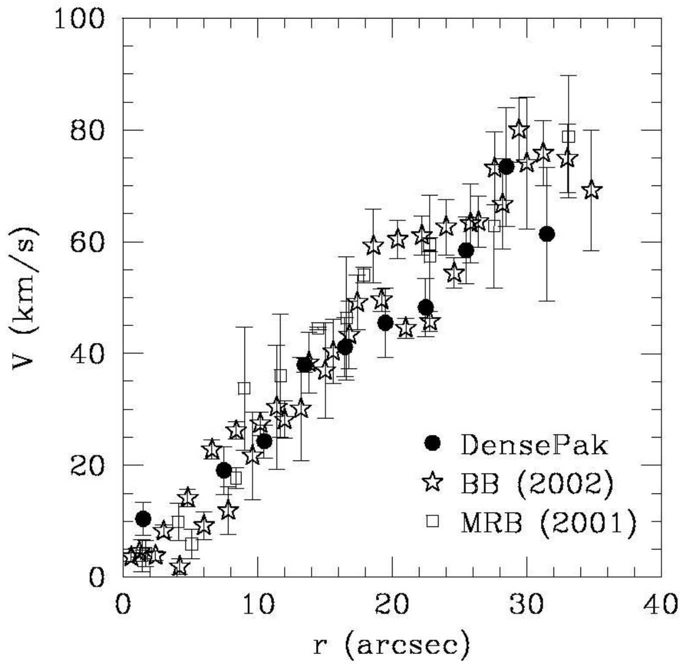

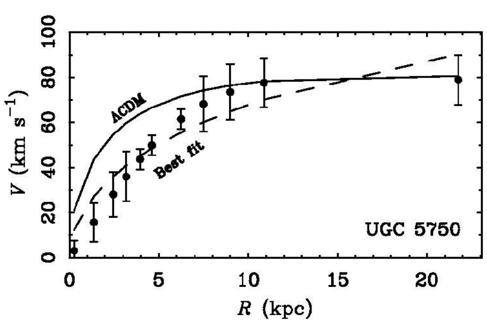

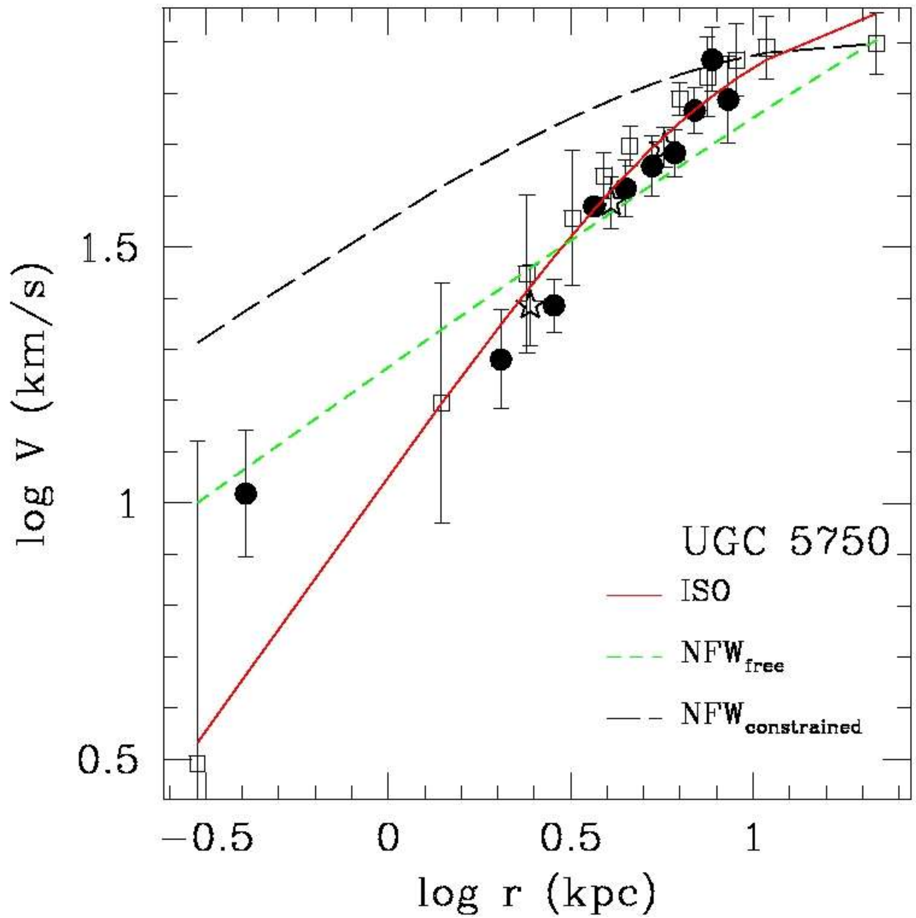

ΛCDM has problems on galaxy scales

cuspy halos

lots of satellites

Kuzio de Naray et al. (ApJ, soumis)

Galaxy formation in ΛCDM

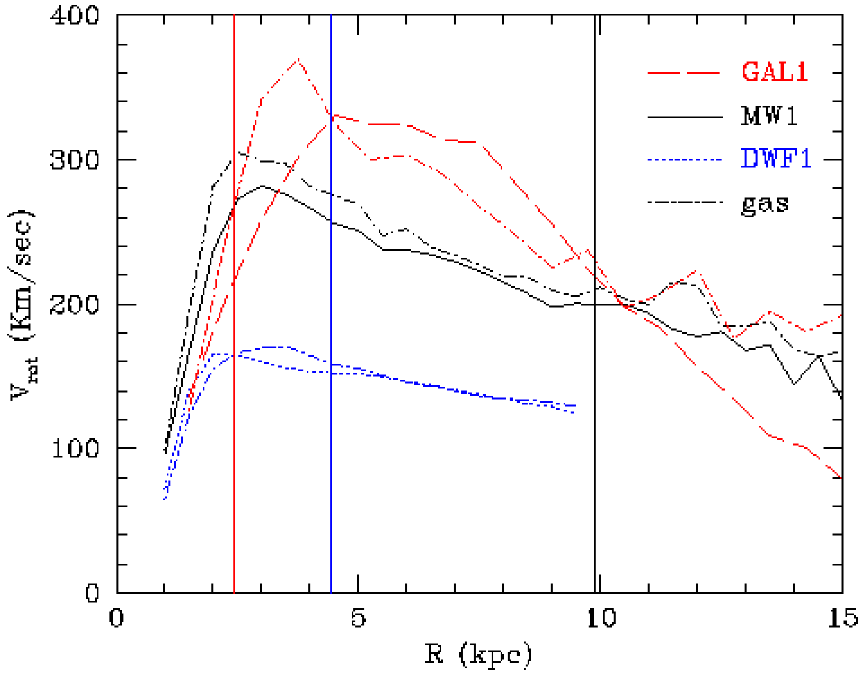

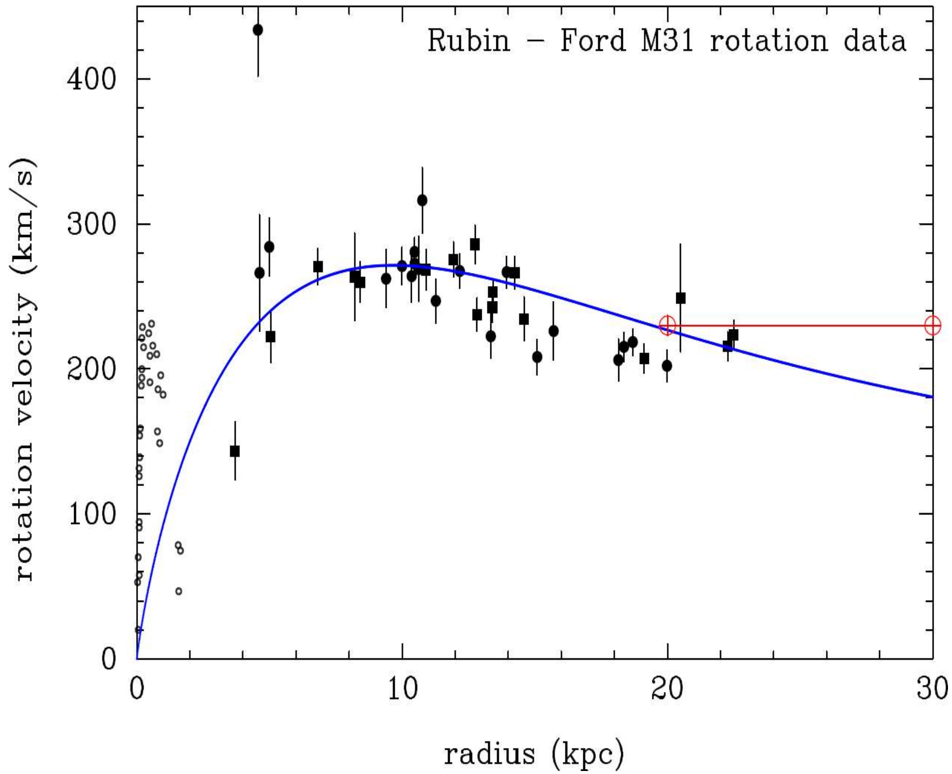

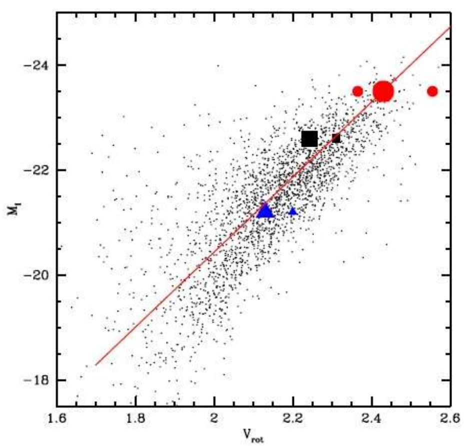

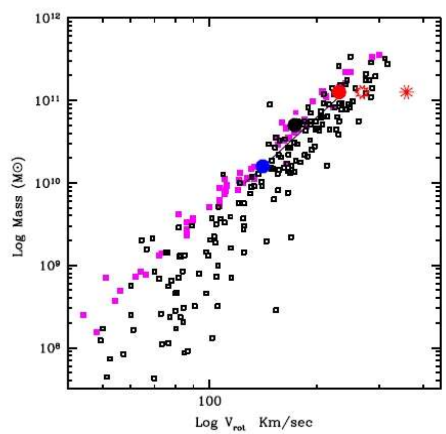

Feedback helps:

TF-relation zero point OK, but halos still too concentrated...

re-calculation on smaller scales to get it “right” Governato et al. 2005/6

What to expect ?

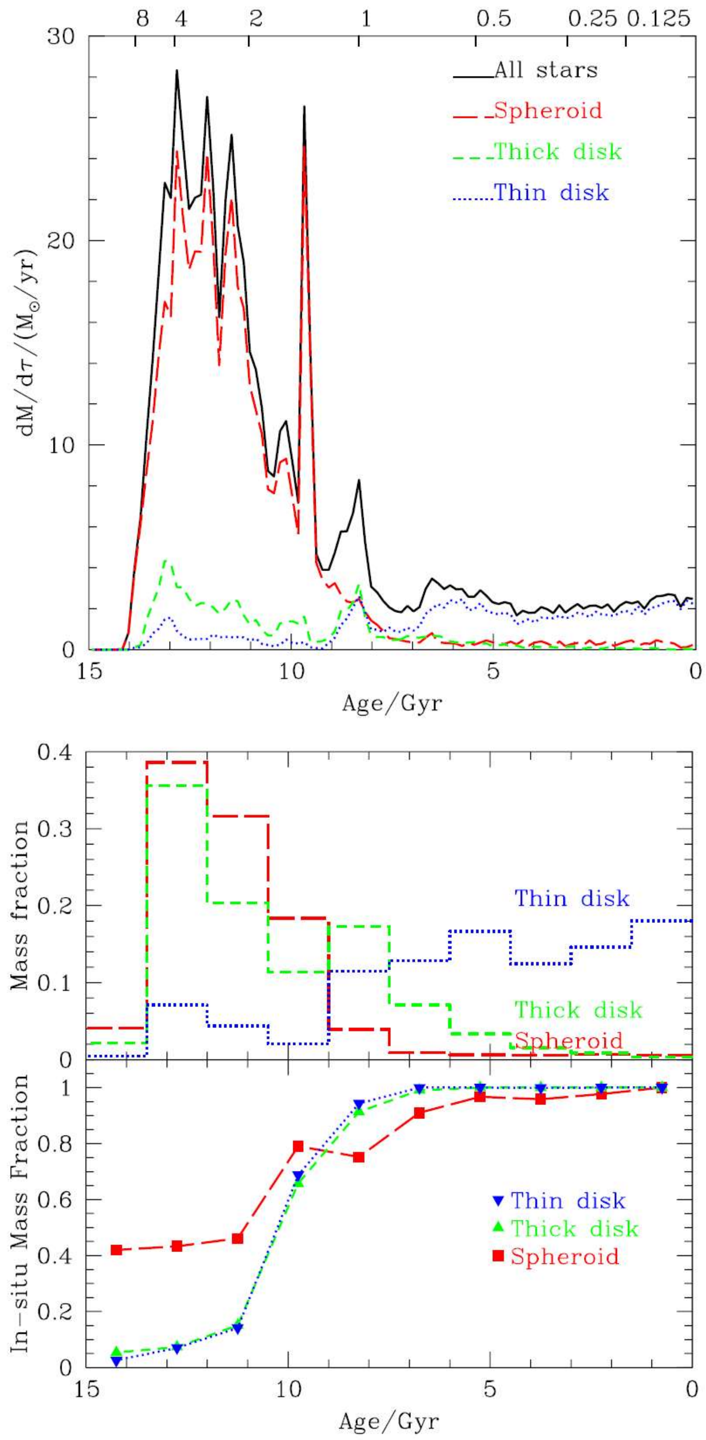

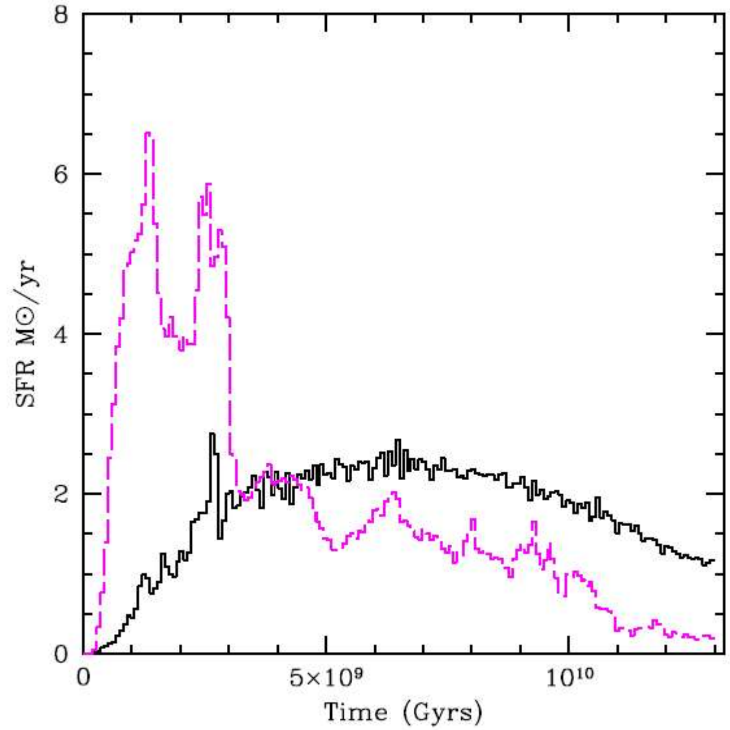

Figure 13. Galaxy DWF1: SFH including all stars within 4 R_z and R_d from the disk plane for two runs. Solid line: ϵSN=0.6, long dashed: no feedback, no UV. The addition of feedback smooths out the SF peaks otherwise present at high redshift and during the last major merger event at z=2.3. Feedback delays the conversion of gas into stars until gas accumulates and cools in the potential well of the main progenitor.

Abadi et al. 2003 Governato et al. 2006

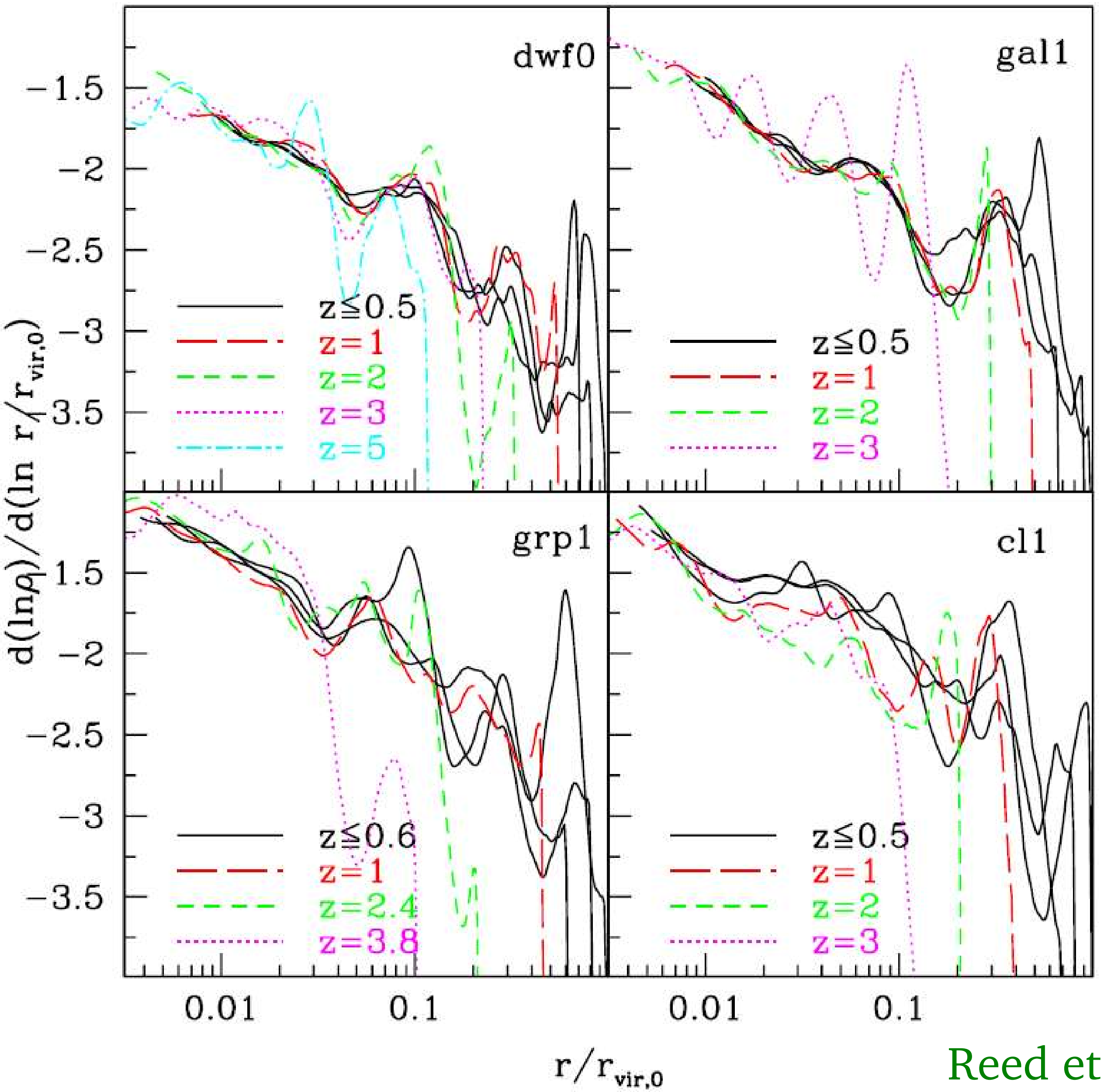

Reed et al. 2005

Figure 6. Evolution of the slope of the density profiles of four haloes plotted against r_{vir} at $z = 0$ in non-comoving (physical) coordinates as in Fig. 3. Mass beyond the virial radius of each epoch is ignored. Note that if plotted simply in terms of r/r_{vir} the haloes would appear to flatten with increased redshift.

Interaction barre - halo

Athanassoula 2002, 2003

Le mécanisme est l'échange
de moment angulaire entre
la barre et le halo

La répartition totale de la
masse se concentre

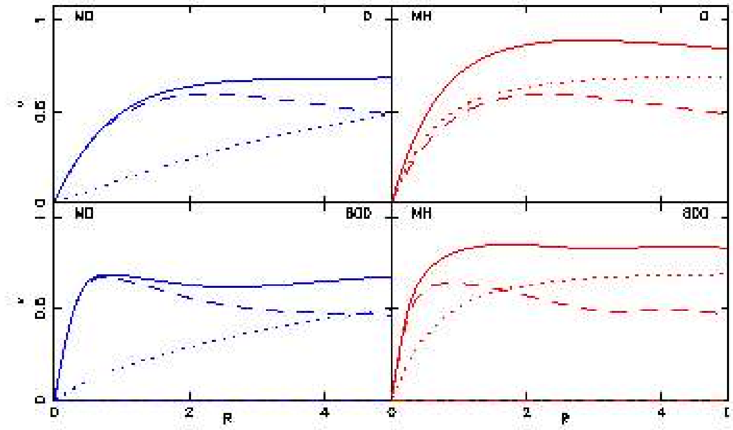

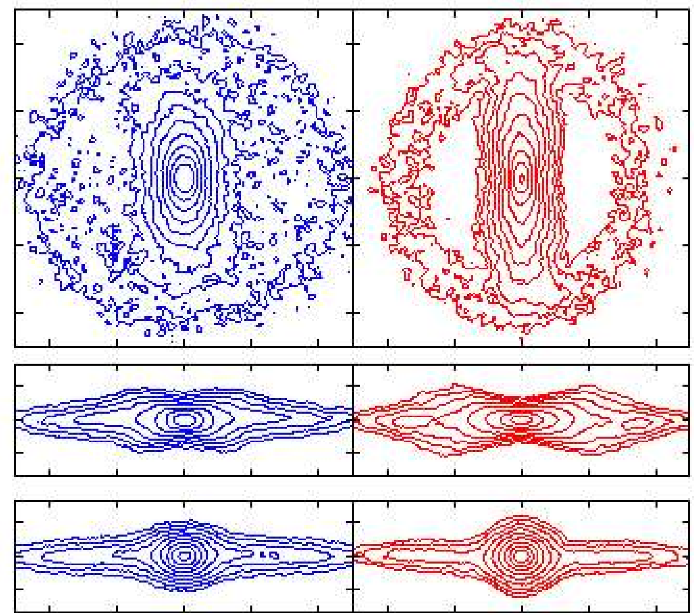

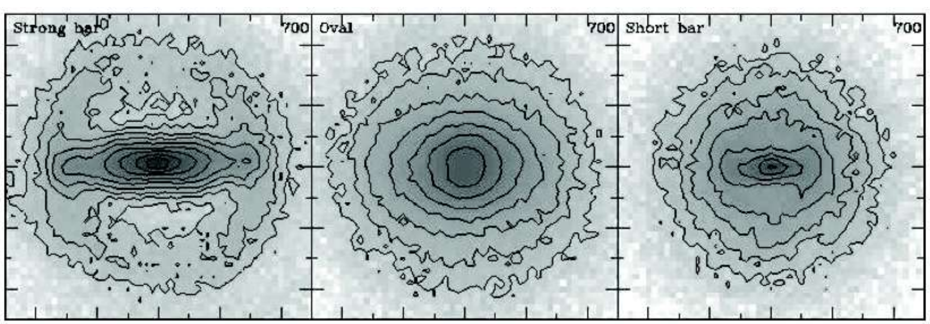

Considerable amount of angular momentum is exchanged

Little angular momentum exchanged

Responsive halo
Hot outer disc

Hot halo

Interaction barre - halo

Bar fraction at high z ?

Jogee et al. (2004)

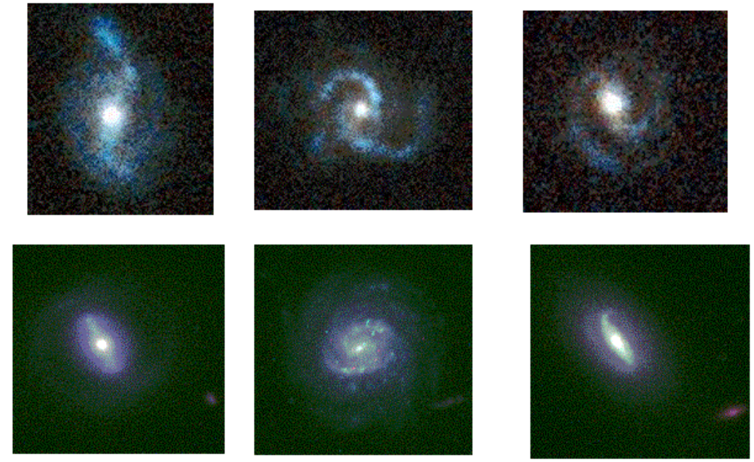

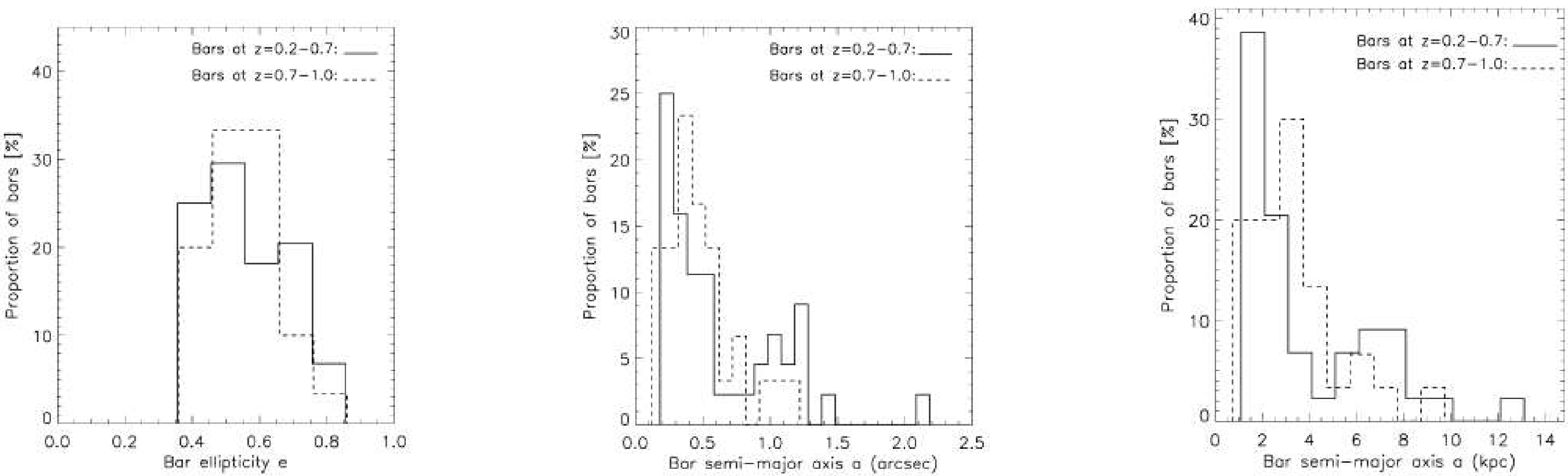

FIG. 2.—Comparison of bars out to look-back times of 8 Gyr. The bar ellipticity e (*left*) and semimajor axis a in arcseconds (*middle*) and kiloparsecs (*right*) are shown for bright ($M_V \leq -19.3$), moderately inclined ($i < 60°$) galaxies at $z \sim 0.2$–0.7 ($T_{back} \sim 2$–6 Gyr) and $z \sim 0.7$–1.0 ($T_{back} \sim 6$–8 Gyr). The bars identified are primarily strong, with $e \geq 0.4$. A large fraction have $a < 0''.5$, and their detection is aided by the narrow ACS PSF.

What to expect ?

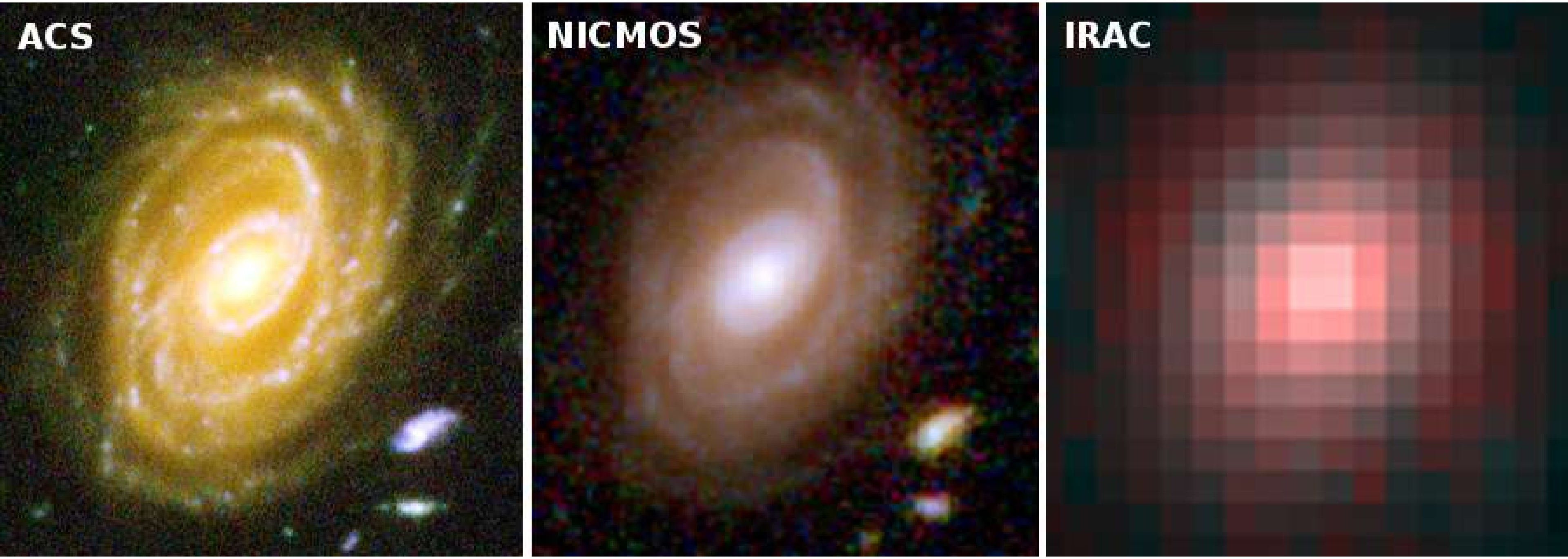

Pixel 0.049 arcsec

Pixel 1.2 arcsec

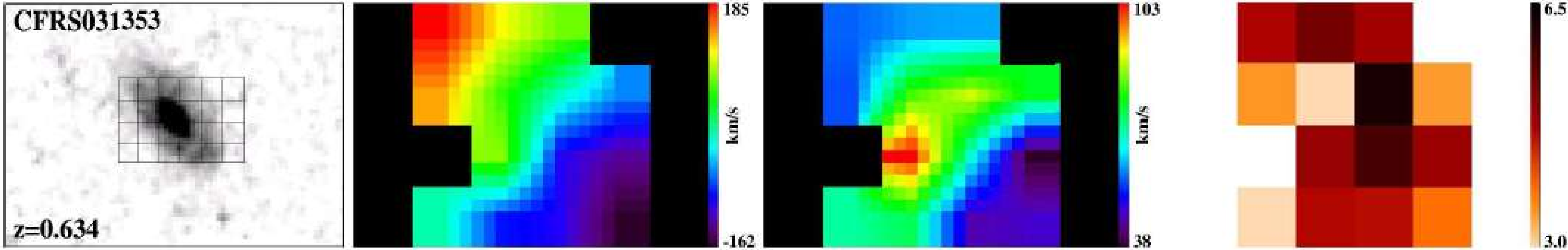

Giraffe – VLT : 0.52 arcsec/pixel; typically 8hrs/exposure

Flores et al. 2005

Resolution problem

Bosma (1978)

For a good rotation curve better have radius/beamsize large (>7 at least, better 15)

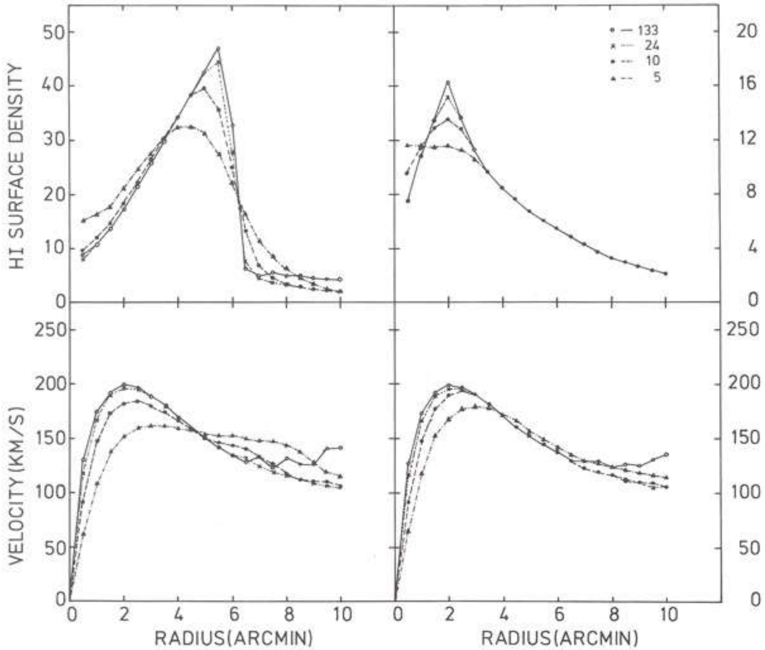

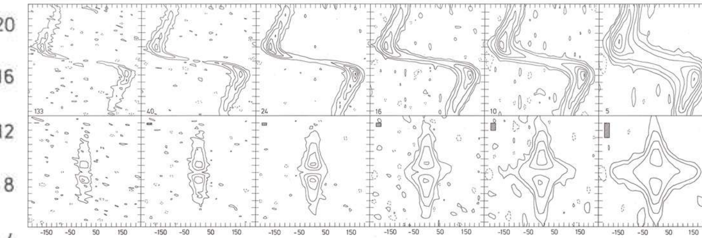

Flores et al. (2004)

12 pixels in radius, at z = 0.22 … and note PA change !

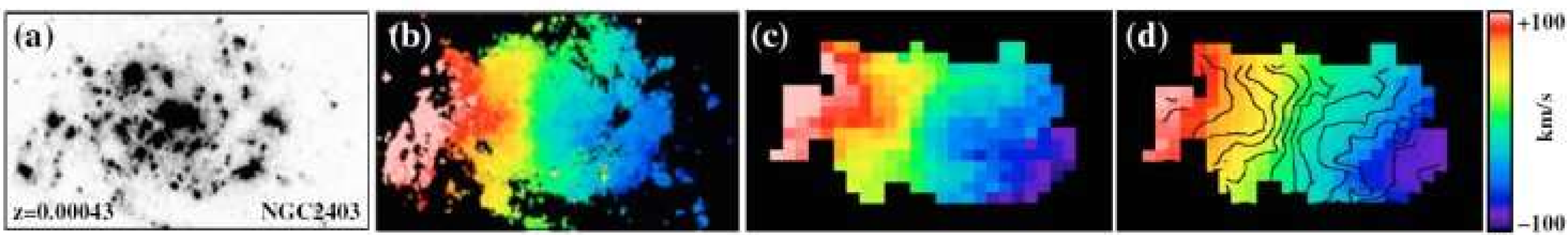

Fig. 1. Example of performed DisGal3D tests with nearby galaxies (here NGC 2403, observed with FanTOmM $R = 27\,000$, Hernandez et al. 2004 and Gach et al. 2003). **a)** Hα map used during the deconvolution process (see text). **b)** VF obtained by FP observation at the mont Megantic Observatory (1.6 arcsec/pix). **c)** Same VF obtained with the galaxy redshifted to $z \sim 0.22$ (0.1 arcsec/pix corresponding to the HST/WFPC2 sampling). **d)** Deconvolved VF obtained by DisGal3D after convolution of the redshifted galaxy by a 0.6 arcsec seeing (see text). Superimposed isovelocities are those from **c)**.

Sans espoir donc ??

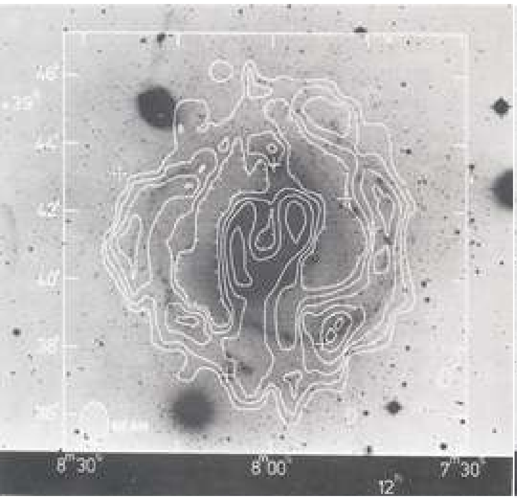

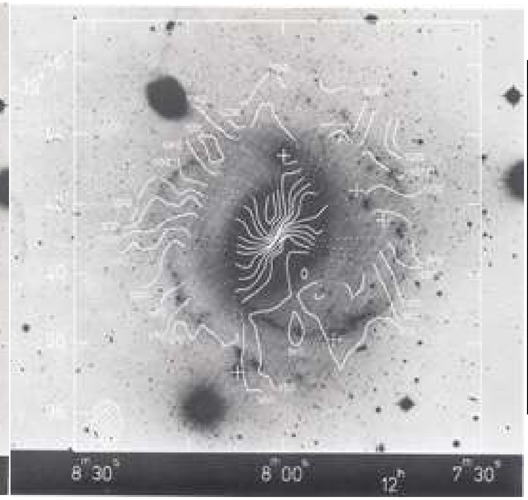

NGC 4151

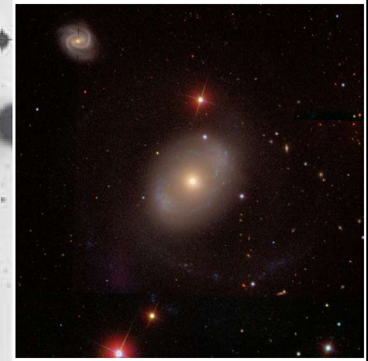

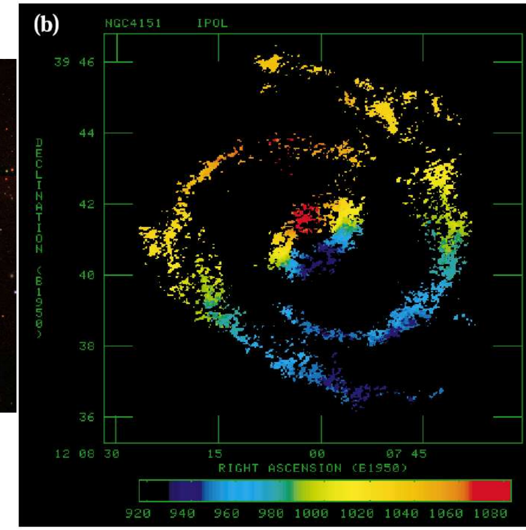

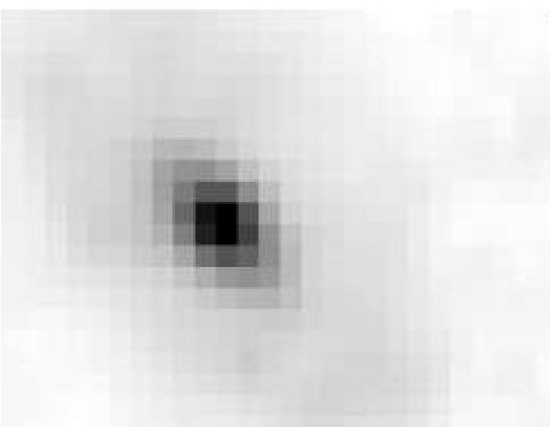

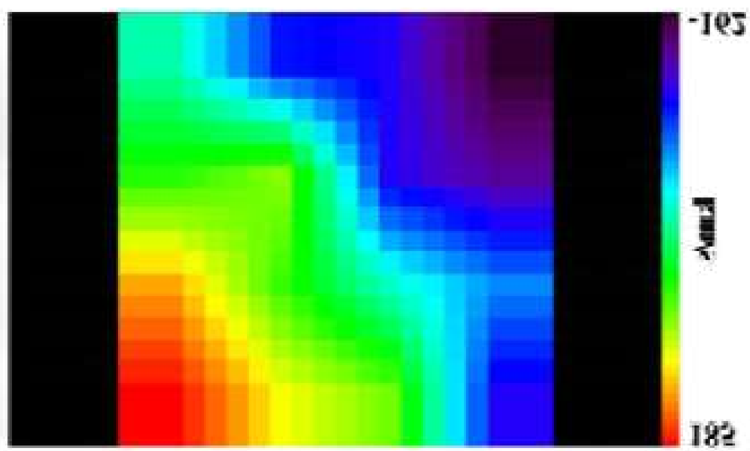

Au moins on pourrait penser que cette galaxie pourrait être ovale/barrée ?

Tully - Fisher results

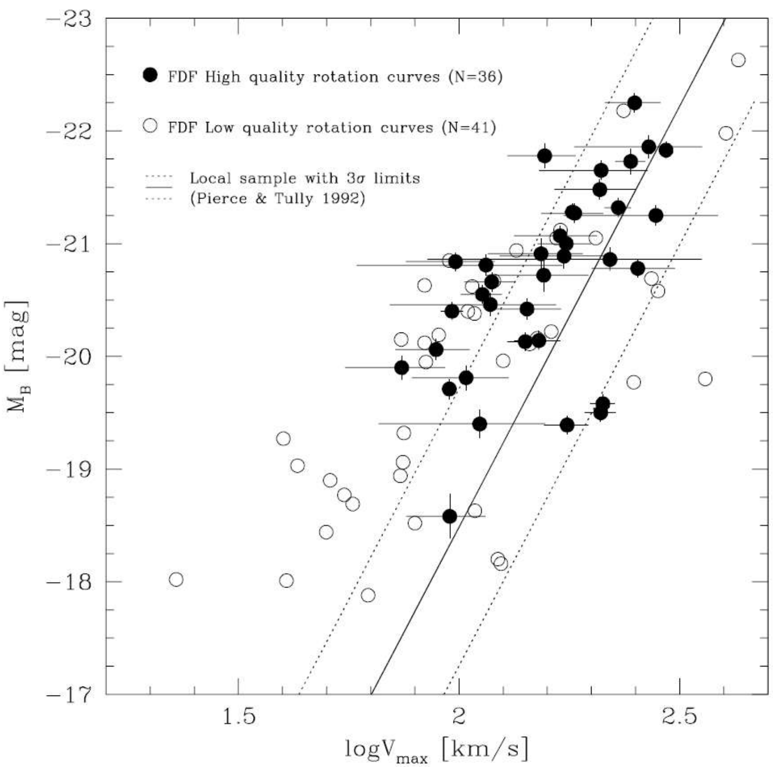

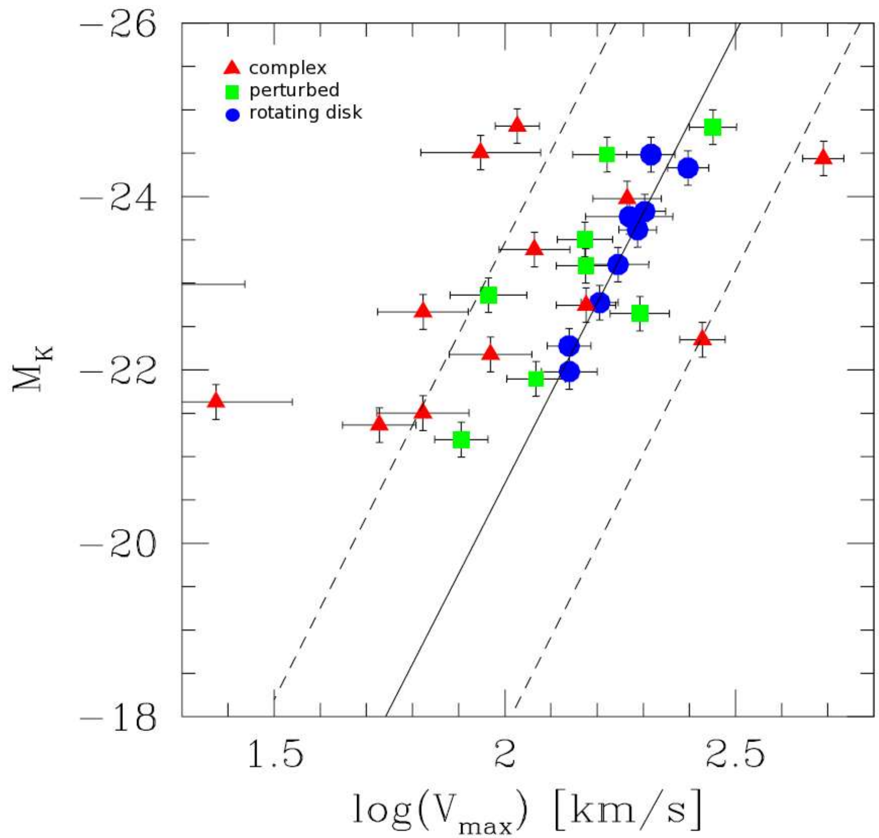

Böhm et al. 2004
use FORS

Flores et al. 2006
use GIRAFFE

Quantitative interpretation of the rotation curves of spiral galaxies at redshifts $z \sim 0.7$ and $z \sim 1$

Fuchs et al. 2004, use a variation of Athanassoula et al. 1987

Strong spiral => Massive disk

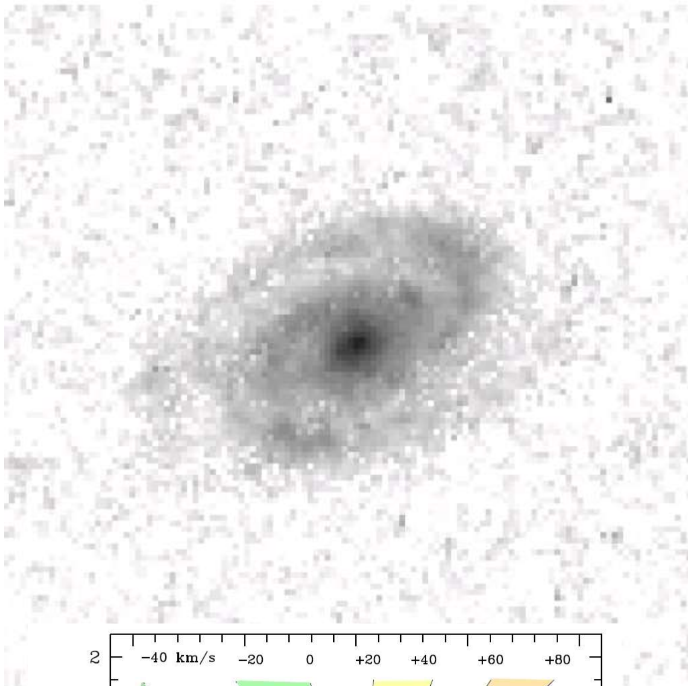

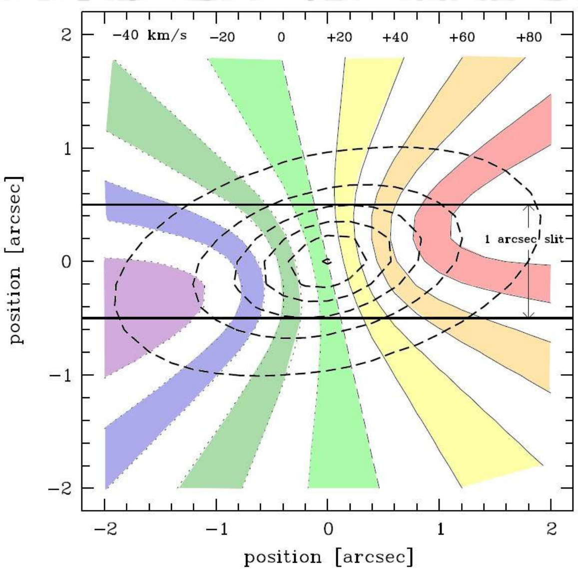

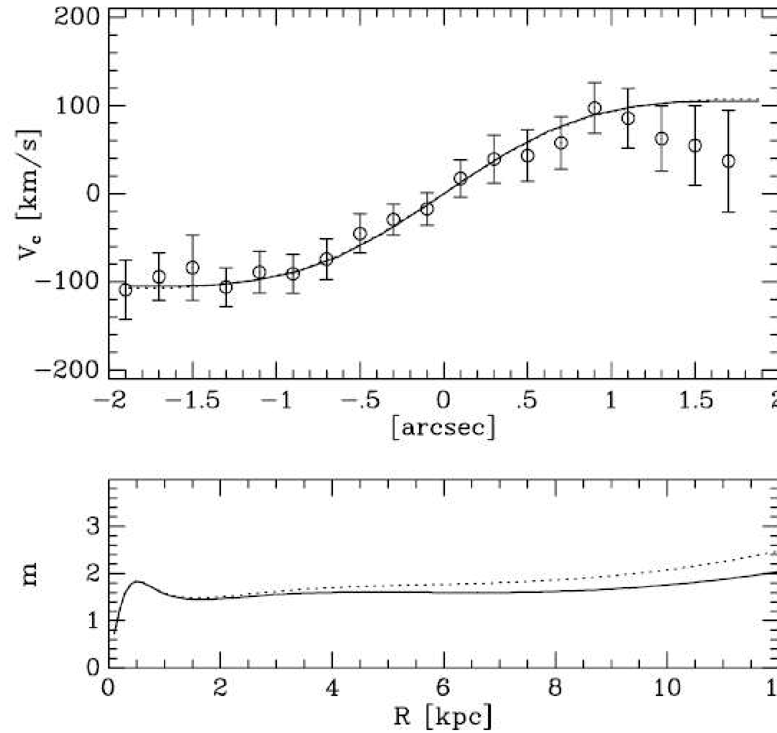

Fig. 3. *Upper panel*: model rotation curves of FDF 2484 fitted to the radial velocity data of Böhm et al. (2004). The solid line is the model without a dark halo, the dotted line shows the corresponding rotation curve when a dark halo component was included. The rotation curves are practically identical. *Lower panel*: expected number of spiral arms in the radial range where spiral structure can be seen. The dotted curve is again for the model with a dark halo included.

Lensing surveys

Koopmans & Treu (2003)
Koopmans – astro-ph/0511121;
Bolton + K + T (3 papers)

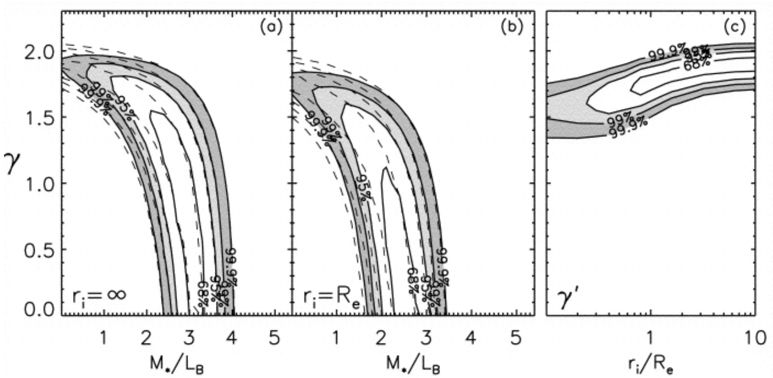

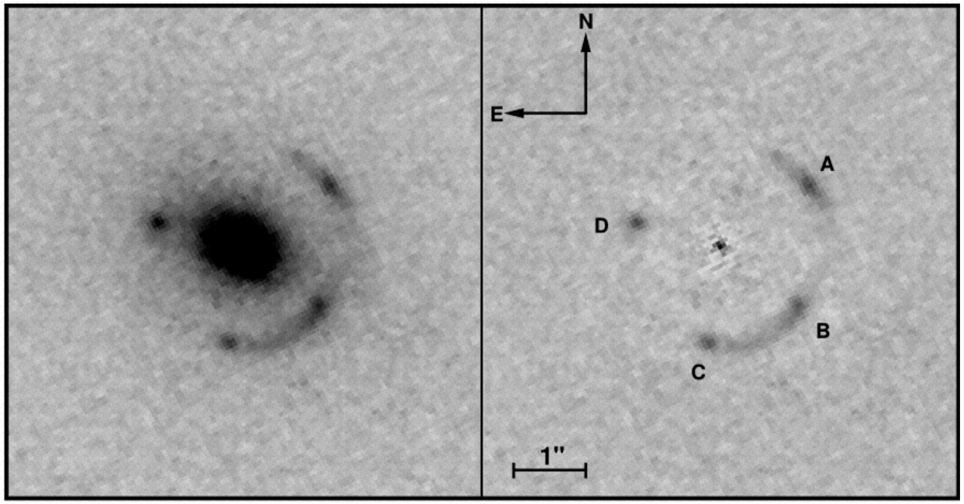

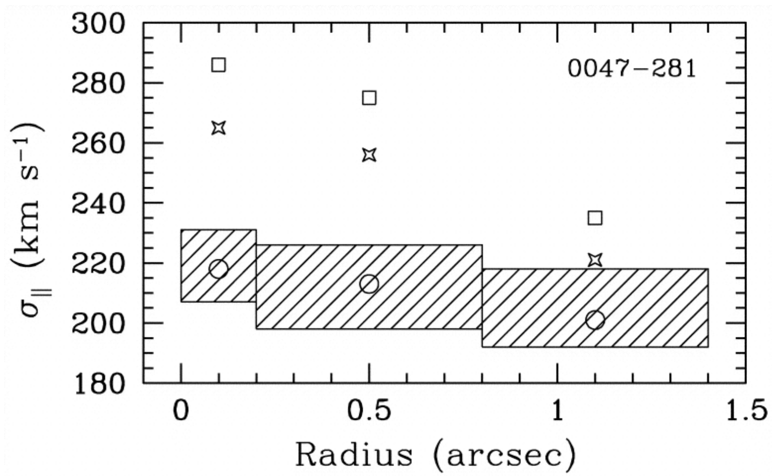

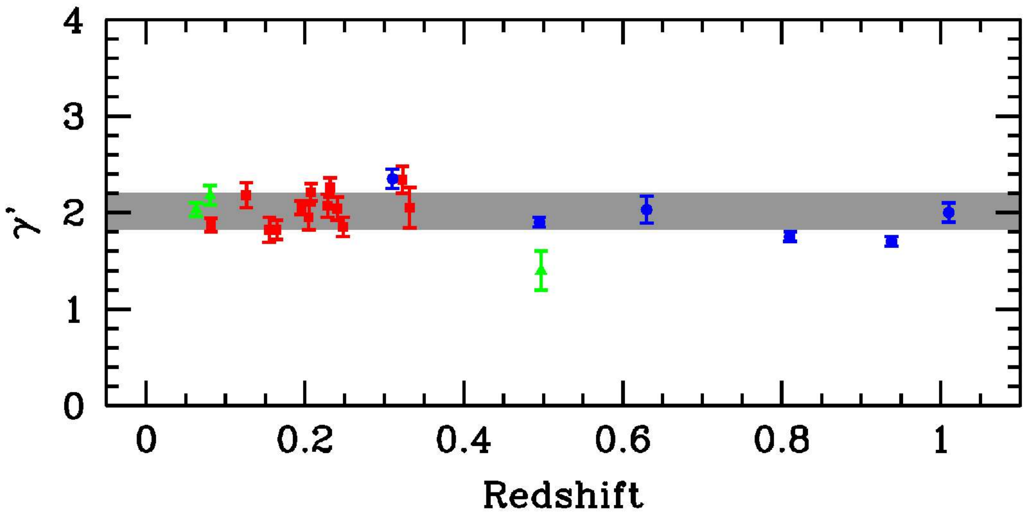

IFU's en 2011

NIRSpec

- Multi-object dispersive spectrograph (MOS)
- Sensitive over the 1-5 micron wavelength range
- 3.4' x 3.4' field of view
- ~0.1" pixels
- R=1000 MOS Mode, 3 gratings cover 1.0-5.0 micron
- R=3000 Integral Field Unit or Long-slit Mode
- R=100 Prism, 0.6-5.0 mm in one exposure
- Capable of observing more than 100 objects simultaneously
- Probably with MEMS (micro-electro-mechanical system) technology, but other options are kept open.

SKA – 100x plus sensible que VLA

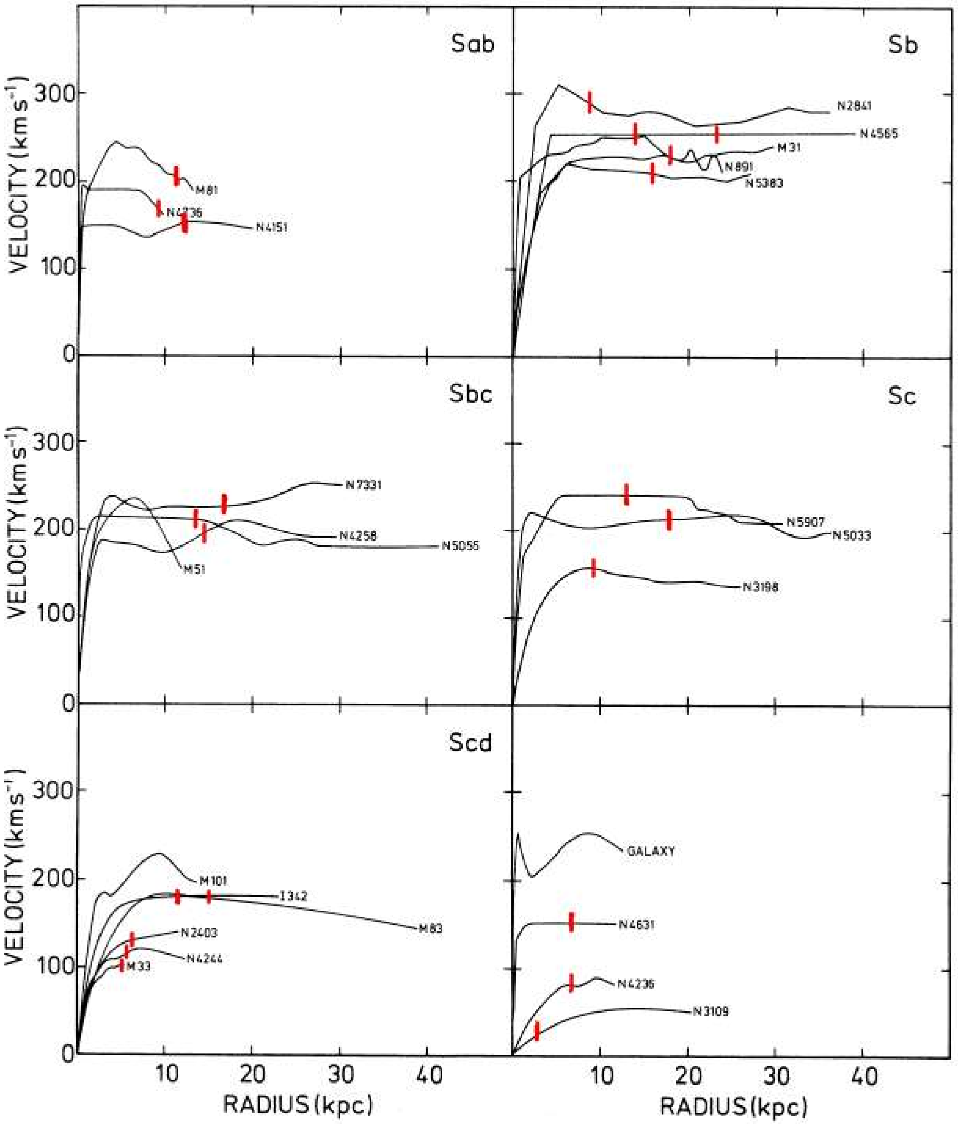

FIG. 3. Rotation curves of 25 galaxies of various Hubble types.

SKA – 100x |

SKA will image galaxies such as M81 and N5055 at z ~ 1

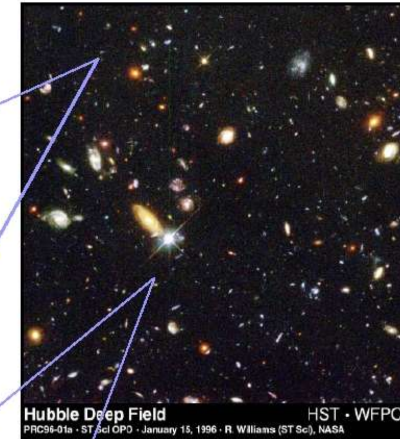

But at a small ratio Radius/Beamsize !

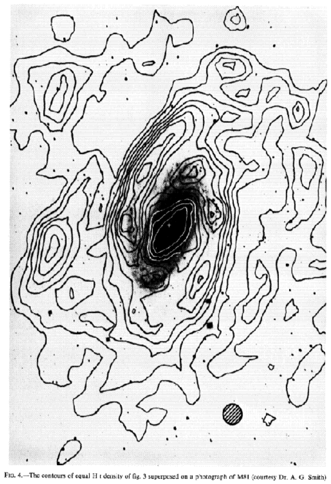

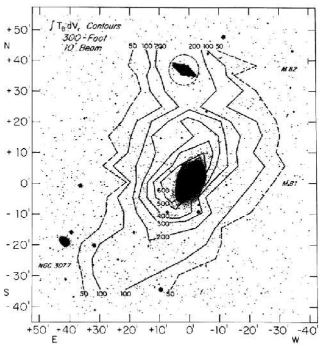

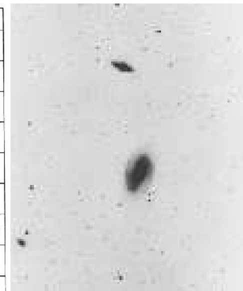

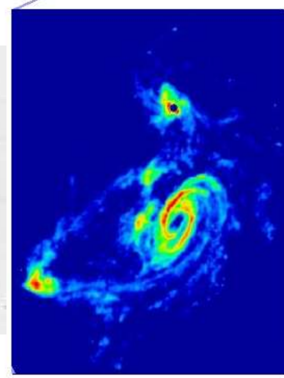

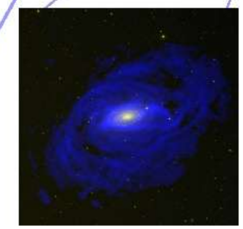

Van der Hulst et al. 2004

Detection limits for HI emission with SKA[a]

z	Frequency (MHz)	T_{sys}[b] (K)	Angular[c] resolution (arcsec)	Linear resolution (kpc)	SB dimming (mag)	Luminosity distance (Gpc)	Lookback time (Gyr)	HI mass[d] limit ($M_\odot$)
0.2	1183.67	50.4	0.52	1.7	0.796	0.972	2.41	6.1×10^8
0.5	946.94	51.4	0.65	4.0	1.486	2.825	5.02	8.7×10^8
1.0	710.20	53.8	0.87	7.0	3.026	6.640	7.73	2.7×10^9
1.5	568.16	57.5	1.09	9.3	4.000	11.02	9.32	7.2×10^9
2.0	473.47	62.7	1.31	11.1	4.796	15.75	10.32	1.5×10^{10}
2.5	405.83	69.6	1.52	12.5	5.469	20.72	11.00	2.6×10^{10}
3.0	355.10	78.3	1.74	13.6	6.052	25.87	11.48	4.3×10^{10}
3.5	315.64	89.3	1.96	14.6	6.566	31.15	11.83	6.7×10^{10}

[a] Assuming $t = 12$ h, $A_e/T_{sys} = 20000$, 2 polarizations and 70% of A_e within 100 km.
[b] Including a contribution from Galactic foreground emission assuming $T_{Gal}(f_{MHz}) = 20\left(\frac{408}{f_{MHz}}\right)^{2.7}$ K.
[c] Fixed array geometry assumed so that resolution scales with wavelength.
[d] Assuming 5 rms and 100 km s^{-1} profile width. At $z = 0.2$ and $z = 0.5$ the galaxies are assumed resolved so here the flux has been added over 8.5 and 1.5 beams respectively.

SKA – 100x plus sensible que VLA

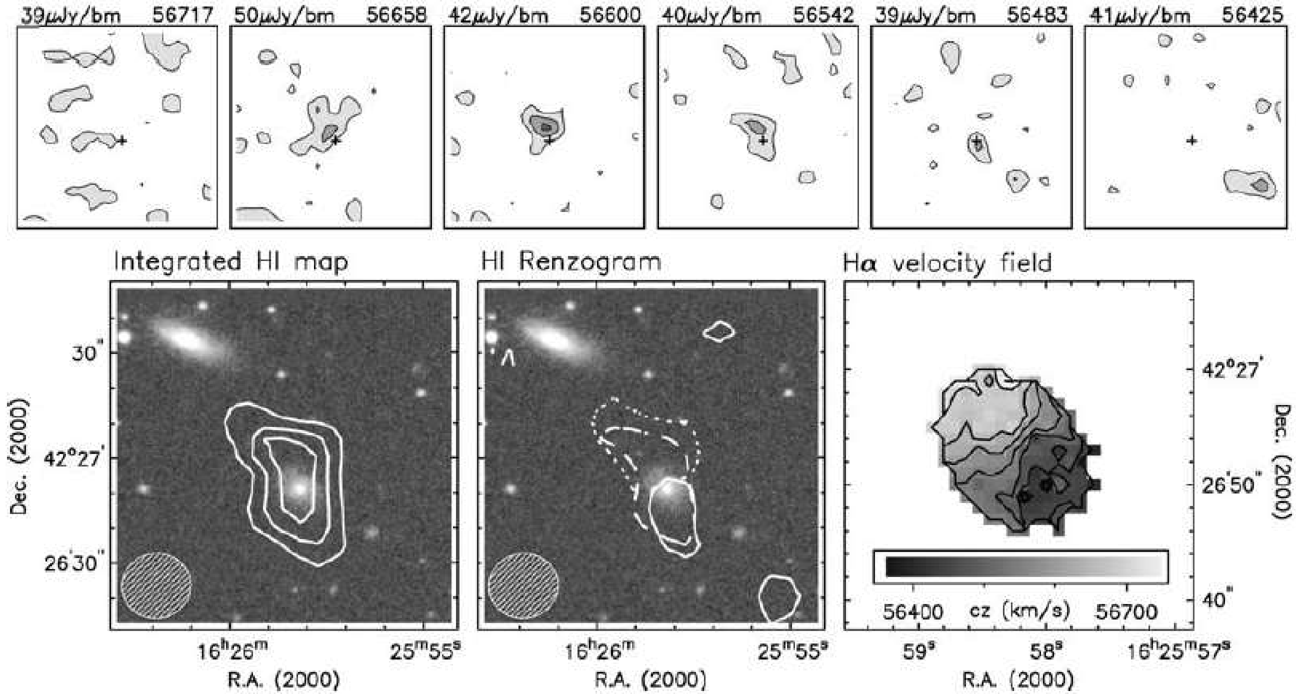

Verheijen & Dwarakanath

Fig. 8. Atomic Hydrogen detected in Abell 2192 at $z = 0.1887$. Upper panels: individual channel maps from the VLA datacube. The

CHAPTER 2. DESIGN GOALS FOR THE ULTRASENSITIVE ARRAY 10

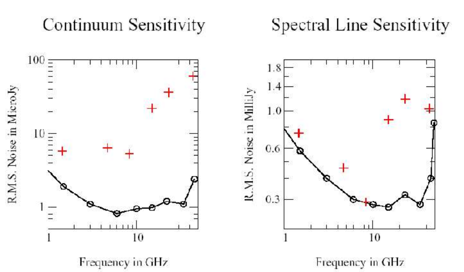

Figure 2.1: The current (+), and projected (o) continuum (left) and spectral line (right) sensitivity (1σ in 12 hours) of the VLA after the Ultrasensitive Array is completed. For the continuum case, a bandwidth of about half the total width of the band is assumed. For the spectral line case, the bandwidth corresponds to a velocity width of 1 km/sec. The width of the '+' symbols demonstrates the approximate range of tuning with the current VLA.

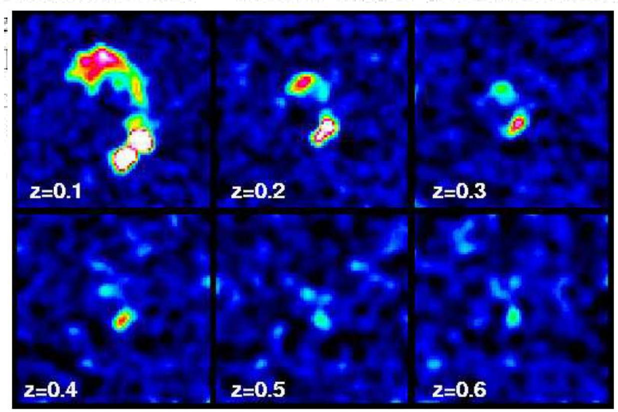

Figure 3.37: The VLA H I Deep Field: the nearby IR luminous merger Arp 299 as a function of redshift (H_0 = 75 km/sec/Mpc, q_0 = 1). The system remains recognizable as a merger out to at $z \gtrsim 0.5$.

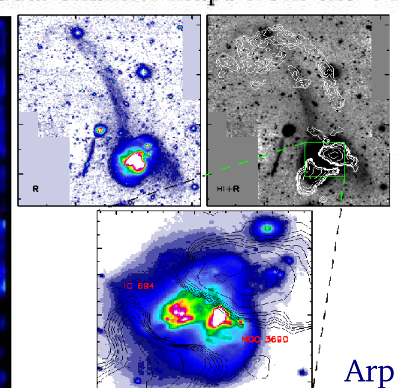

EVLA

Arp 299 z=0.01